

DAM: DUAL ACTIVE LEARNING WITH MULTIMODAL FOUNDATION MODEL FOR SOURCE-FREE DOMAIN ADAPTATION

*Xi Chen*¹

Hongxun Yao^{1*}

*Zhaopan Xu*¹

*Kui Jiang*¹

¹ Harbin Institute of Technology

ABSTRACT

Source-free active domain adaptation (SFADA) enhances knowledge transfer from a source model to an unlabeled target domain using limited manual labels selected via active learning. While recent domain adaptation studies have introduced Vision-and-Language (ViL) models to improve pseudo-label quality or feature alignment, they often treat ViL-based and data supervision as separate sources, lacking effective fusion. To overcome this limitation, we propose Dual Active learning with Multimodal (DAM) foundation model, a novel framework that integrates multimodal supervision from a ViL model to complement sparse human annotations, thereby forming a dual supervisory signal. DAM initializes stable ViL-guided targets and employs a bidirectional distillation mechanism to foster mutual knowledge exchange between the target model and the dual supervisions during iterative adaptation. Extensive experiments demonstrate that DAM consistently outperforms existing methods and sets a new state-of-the-art across multiple SFADA benchmarks and active learning strategies.

Index Terms— Active learning, source-free domain adaptation, Vision-and-Language model

1. INTRODUCTION

Deep neural networks often exhibit limited generalization to unseen domains due to distributional shift between training (source) and target data. This challenge is prevalent in applications such as autonomous driving, remote sensing, and medical imaging. Unsupervised domain adaptation (UDA) [1, 2] addresses this shift by aligning feature distributions across domains; however, its dependence on source data introduces privacy concerns [3] and logistical challenges. Source-free domain adaptation (SFDA) [4–6] offers a more practical alternative by adapting a pre-trained source model without access to the original data, though this constraint makes adaptation more challenging. Allowing minimal labeling effort on the target data can yield substantial gains further for SFDA, motivating the study of source-free active domain adaptation (SFADA) [7–9].

Meanwhile, Vision-and-Language (ViL) foundation models, e.g., CLIP [10] and ALIGN [11] have demonstrated remarkable zero-shot generalization and potential for downstream knowledge transfer. Their rich multimodal representations are promising for bridging domain gaps, especially in low-data regimes, e.g., via prompt tuning [12] or adapter modules [13]. This prompts a key research question: *Under a fixed labeling budget, how can we best leverage ViL models to improve the adaptation of source-domain-pretrained models to a target domain?* Although several studies [1, 2, 14] have primarily incorporated ViL models for enhanced pseudo-labeling or feature alignment, they often treat the ViL model and data as separate sources of pseudo-supervision. For instance, a straightforward combination that merely integrates active samples [7] with a ViL-based method like DIFO [14] yields only marginal gains (+1.1%/0.4% on Office-Home/VisDA-C datasets)—significantly lower than the +7.5%/8.9% improvement achieved by methods that rely solely on data pseudo-supervision without ViL components [7]. This result underscores that effectively leveraging ViL models requires more sophisticated interaction mechanisms beyond simple combination.

To address this combination gap, we propose Dual Active learning with Multimodal (DAM) foundation model. As shown in Fig. 1a, our approach augments the target model with auxiliary supervision from a ViL model throughout adaptation. However, since the ViL model is source-agnostic and lacks task-specific knowledge, its representations must be carefully activated to provide reliable guidance. To this end, beyond conventional active sample supervision [7, 15, 16], we design a more stable ViL-based signal by prompt-tuning with those active samples, forming a Dual-Focused active Supervision (DFS). Furthermore, to fully exploit both supervisions, we introduce an Alternative Distillation (ADL) strategy that facilitates bidirectional knowledge transfer between the supervisions and the target model throughout adaptation. This enables mutual enhancement by exchanging the ViL model’s generalization capacity with the target-specific representations learned by the target model, thereby improving adaptation performance for both.

In summary, our main contributions are as follows: (1) We propose DAM, a novel framework that integrates ViL-based supervision with active learning to construct a dual supervi-

*Corresponding author.

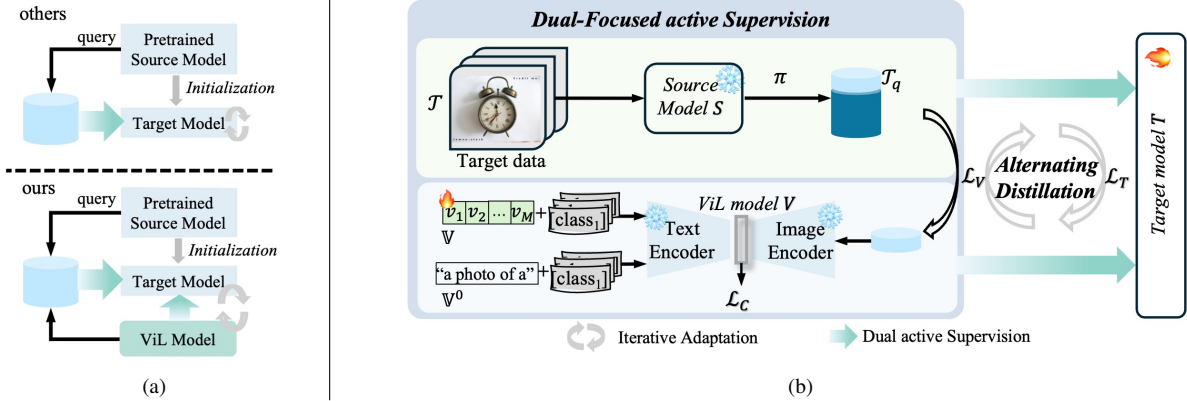


Fig. 1: (a): Comparison: conventional SFADA methods [7, 8, 15] vs. our approach with ViL model supervision. (b): Overview of DAM. The target samples \mathcal{T} are first sent to source model S , selecting \mathcal{T}_q with strategy π . ViL model is tuned for auxiliary active supervision, forming *Dual-focused active Supervision*. Moreover, *Alternating Distillation* enables bidirectional knowledge transfer for target model adaptation.

sory signal, significantly enhancing SFADA under a limited budget. (2) We design a DFS mechanism to activate task-aware ViL supervision using selected target samples, and an ADL protocol to enable mutual knowledge exchange between the target model and the dual supervisions. (3) Extensive experiments show that DAM sets new state-of-the-art results across multiple benchmarks and active learning strategies.

2. METHODOLOGY

In the context of SFADA, a source model S is first pretrained on a labeled source dataset $\{(x_i, y_i)\}_{i=1}^m$ spanning C classes. The goal of SFADA is to select a subset of labeled samples \mathcal{T}_q from unlabeled target data $\mathcal{T} = \{x'_i\}_{i=1}^n$ within a labeling budget B , using an active query strategy π , such that the target risk of the target model T on \mathcal{T} is minimized. The target model T is initialized with source parameters $T = S$, and adaptation is performed without access to the source data S . Following [7], we adopt a one-shot query strategy, where all queried samples \mathcal{T}_q are selected according to raw source model S under the constraint $|\mathcal{T}_q| = \rho|\mathcal{T}|$, with $\rho \in (0, 1)$. The labels of these samples are obtained from an oracle and subsequently used for model adaptation.

In this work, we incorporate a ViL model V as an auxiliary source of prior knowledge for T . Let f^I represent the image features extracted by the frozen image encoder of V . The corresponding text embeddings are derived from a set of learnable category prompts $\{\mathbb{V}_k\}_{k=1}^C$, where each prompt \mathbb{V}_k is structured as $\{v_1, v_2, \dots, v_m, c_k\}$. These prompts are initialized using the template \mathbb{V}_k^0 : "a photo of a [c_k]" and are fed into the frozen text encoder to obtain text embeddings $\{\mathbf{w}_k\}_{k=1}^C$ such that $\mathbf{w}_k = \text{Enc}_t(\mathbb{V}_k)$. The prediction probability for class k given an input image x is computed as:

$$p_V^{(k)}(x) = \frac{\exp(\text{sim}(f^I, \mathbf{w}_k)/\tau)}{\sum_{i=1}^C \exp(\text{sim}(f^I, \mathbf{w}_i)/\tau)}, \quad (1)$$

where $\text{sim}(\cdot, \cdot)$ denotes cosine similarity, and τ is a learned temperature parameter within ViL model. Throughout the adaptation, both the text and image encoders of the ViL model are frozen; only the category prompts are optimized to specialize the model to the target domain.

The overall architecture is illustrated in Fig. 1b.

2.1. Dual-Focused Active Supervision (DFS)

In addition to conventional data supervision from the labeled subset \mathcal{T}_q under different sampling strategies π , we incorporate supervisory signals from the ViL model using the same set. As the query ratio ρ is small, to effectively adapt the ViL model to the target domain and prevent overfitting, we follow a supervised prompt learning strategy [17] to preserve the model's foundational generalization capabilities. This design choice is grounded in the ViL model's inherent capacity for robust multimodal alignment. Specially, after the one-shot active sample query for \mathcal{T}_q , the context vectors \mathbb{V} are optimized by minimizing the following Cross-Entropy loss \mathcal{L}_{ce} and regularization loss \mathcal{L}_{kg} :

$$\mathcal{L}_C = \mathcal{L}_{ce} + \mathcal{L}_{kg} = \mathbb{E}_{x \in \mathcal{T}_q} \text{CE}(\mathbf{e}_y \| p_V(x)) + \frac{1}{C} \sum_{k=1}^C \|\mathbf{w}_k - \mathbf{w}_k^0\|_2^2, \quad (2)$$

where \mathbf{e}_y denotes the one-hot vector of the ground-truth label y (i.e., $\mathbf{e}_y \in \{0, 1\}^C$ and $\mathbf{e}_y(k) = 1$ if $k = y$), and \mathcal{L}_{kg} regularize the textual embeddings \mathbf{w}_k by anchoring them to their original general-purpose counterparts $\mathbf{w}_k^0 = \text{Enc}_t(\mathbb{V}_k^0)$ to maintain its generalization.

2.2. Alternating Distillation (ADL)

To further use the dual-path supervision signals for target model adaptation to unlabeled target data, we propose an

alternating distillation mechanism that aims to combine the task-specific discriminative knowledge from the target model and labeled samples \mathcal{T}_q with the generalizable cross-modal knowledge from the ViL model.

Specifically, the data supervision is utilized in this distillation process via a direct weighting scheme that emphasizes reliable samples \mathcal{T}_q with oracle annotations while down-weighting samples with uncertain pseudo-labels. The unified mutual teacher framework provides supervision in the following manner: for a student model $A \in \{T, V\}$ taught by teacher model $B \in \{V, T\}$, we define the teacher’s output distribution and sample weights $\mathcal{W}(\cdot)$ as:

$$(\tilde{p}_{A \leftarrow B}, \mathcal{W}) = \begin{cases} (e_y, \beta_q), x \in \mathcal{T}_q \text{ with label } y, \\ (\text{F}(B(x)/\tau_B), \beta), x \in \mathcal{T} \setminus \mathcal{T}_q, \end{cases} \quad (3)$$

where $\text{F}(\cdot)$ is Softmax(\cdot) operation, $\beta_q \geq \beta > 0$ are hyperparameters controlling the weight contribution. The student’s prediction is given by $p_A^{\tau_A}(x) = \text{F}(A(x)/\tau_A)$. Note that hard pseudo-labeling emerges as a special case when $\tau_B \rightarrow 0$, which reduces the teacher’s distribution to a one-hot vector.

2.2.1. Distillation from $T \rightarrow V$

During each epoch, we select the top- N most confident samples per class from the target model’s predictions: $X_{\text{top}} = \bigcup_{y \in \mathcal{Y}_t} \text{top-}N \text{ by } \max_k T^{(k)}(x) \text{ within class } y$ and enable task-specific knowledge distillation to the ViL model through their associated soft labels $T(x)$ with $\tau_V = \tau_T = 1$ by:

$$\mathcal{L}_{\text{dist}}^{V \leftarrow T} = -\mathbb{E}_{x \in X_{\text{top}} \cup \mathcal{T}_q} \mathcal{W}(x) \text{CE}(\tilde{p}_{V \leftarrow T}(x) || p_V^{\tau_V}(x)). \quad (4)$$

2.2.2. Distillation from $V \rightarrow T$

Conversely, since the ViL model outputs multimodal cosine similarities as predictions, the hard labels produced by the ViL model are used as pseudo-labels for unlabeled samples $\mathcal{T} \setminus \mathcal{T}_q$ to supervise the adaptation of the target model. The distillation loss for the target model is formulated as:

$$\mathcal{L}_{\text{dist}}^{T \leftarrow V} = -\mathbb{E}_{x \in \mathcal{T}} \mathcal{W}(x) \text{CE}(\tilde{p}_{T \leftarrow V}(x) || p_T^{\tau_T}(x)), \quad (5)$$

where $\tau_T = 1$ and $\tau_V \rightarrow 0$.

Following prior works [4, 14, 18], we incorporate entropy minimization and diversity regularization loss terms to guarantee the unambiguous and balanced classes:

$$\mathcal{L}_{\text{ent}} = \mathbb{E}_{x \in \mathcal{T}} \text{CE}(p_T(x) || p_T(x)), \quad (6)$$

$$\mathcal{L}_{\text{div}} = \sum_{k=1}^C \hat{p}_k \log(\hat{p}_k) = \text{KL}(\hat{p}, \frac{1}{C} \mathbb{1}(C)) - \log C, \quad (7)$$

where $\hat{p} = \mathbb{E}_{x \in \hat{\mathcal{X}}_t} [p_T(x)]$ represents the average output embedding for the whole target dataset, KL is the KL distance, and $\mathbb{1}(C)$ is a vector of ones with dimension C .

The overall training losses are then defined as:

$$\mathcal{L}_T = \mathcal{L}_{\text{dist}}^{T \leftarrow V} + \mathcal{L}_{\text{ent}} + \mathcal{L}_{\text{div}}, \quad (8)$$

$$\mathcal{L}_V = \mathcal{L}_{\text{dist}}^{V \leftarrow T} + \mathcal{L}_{\text{kg}}. \quad (9)$$

After training, the ViL model is discarded, and only the target model is used for inference.

3. EXPERIMENT

3.1. Datasets

We evaluate our method on three benchmarks: (1) Office [19]: A small-scale dataset across Amazon, Dslr, and Webcam domains; (2) Office-Home [20]: A medium-scale dataset that is distributed across four domains: Art, Clipart, Product and Real-World; (3) VisDA-C [21]: A large-scale dataset designed for Synthetic-to-Real adaptation.

3.2. Baselines

Our method is evaluated against comprehensive baselines, spanning five categories (1) Source(model)-only and zero-shot CLIP with ViT-B/32 backbone (ZS-C-B32), where we use the standard prompt “a photo of a [class]”; (2) Unsupervised DA (UDA) methods; (3) Source-free DA (SFDA) approaches; (4) Active DA (ADA) methods; and (5) Source-free active DA (SFADA) techniques.

3.3. Implementation

Our implementation for training source and models follows the established training pipeline of prior works [4, 7, 18]. Specifically, ResNet-50 [22] is used for Office and Office-Home datasets, while ResNet-101 [22] is employed for VisDA-C. For the ViL model component, we use the CLIP model [10] with a ViT-B/32 image encoder [23] across all experiments. The hyperparameters in Eq. 3 are set as $\beta_q = 3$ and $\beta = 0.3$. The context vector length m of prompts is set to 16, and the X_{top} set is constructed with $N = 16$. In DFS, the prompts are optimized using SGD with a base learning rate of 2×10^{-3} , incorporating a warmup strategy starting at 1×10^{-5} for the first epoch and followed by cosine annealing over 50 epochs. In ADL, prompt learning rate is maintained at 2×10^{-3} . All experiments were run on a single NVIDIA RTX 4090 GPU and conducted with a labeling budget of $\rho = 5\%$ unless otherwise specified.

3.4. Main Results

Table 1 demonstrates the superior performance of DAM across multiple benchmarks. Comparative analysis with BIAS [9]—a plug-and-play framework that aligns distributions of inactive and active samples—reveals consistent improvements across all datasets and base methods. Specifically,

Table 1: Performance (%) on three datasets with a 5% labeling budget. SF: source-data-free; ViL: use ViL models; 'OH': Office-Home dataset. \dagger : Reimplemented using official code with source models identical to ours.

Categories	SF	Method	ViL	Office	OH	VisDA-C
Zero-shot	✓	Source-only ZS-C-B32 [10]	✗ ✓	77.2 79.5	58.7 72.2	46.9 87.2
	✗	RADA-prompt [2] DAPL [1]	✗ ✓	91.6 -	72.9 74.5	90.5 86.9
SFDA	✓	CPGA [24] SHOT [4] A2Net [5] GRAPE [18] DIFO-C-B32 \dagger [14]	✗ ✗ ✗ ✗ ✓	89.9 88.6 90.1 91.6 92.6	71.6 71.8 72.8 75.4 76.3	86.0 82.4 84.3 89.2 90.1
		CLUE [25] EADA [26] DUC [27] CA-ADA [28]	✗ ✗ ✗ ✗	89.5 93.2 -	72.5 76.7 78.0 79.3	- 88.3 88.9 -
ADA	✗	SQAdapt [8] ELPT [15] +DAM CoreSet [16] +BIAS [9] +DAM MHPL [7] +BIAS [9] +DAM	✗ ✗ ✓ ✗ ✗ ✓ ✗ ✗ ✓	- 92.8 93.5 90.3 91.0 93.4 93.2 93.6 94.1	77.8 77.0 81.9 75.2 76.8 83.9 79.3 80.3 82.0	91.3 89.2 91.9 85.9 88.2 92.0 91.3 91.1 92.0
SFADA	✓	SQAdapt [8] ELPT [15] +DAM CoreSet [16] +BIAS [9] +DAM MHPL [7] +BIAS [9] +DAM	✗ ✗ ✓ ✗ ✗ ✓ ✗ ✗ ✓	- 92.8 93.5 90.3 91.0 93.4 93.2 93.6 94.1	77.8 77.0 81.9 75.2 76.8 83.9 79.3 80.3 82.0	91.3 89.2 91.9 85.9 88.2 92.0 91.3 91.1 92.0

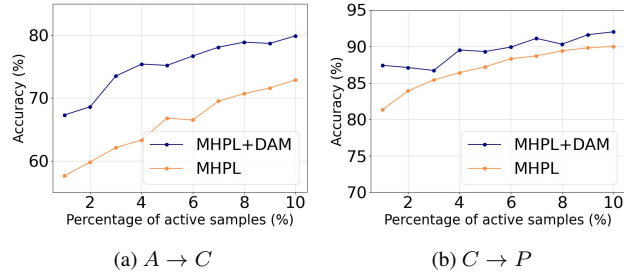


Fig. 2: Ablation study of model performance with DAM across different labeling quotas for active learning on the transfer task (a) $A \rightarrow C$ and (b) $C \rightarrow P$ of Office-Home dataset.

Table 2: Ablation study of \mathcal{L}_C and \mathcal{L}_V on two transfer tasks in the Office-Home dataset.

Method	\mathcal{L}_C	\mathcal{L}_V	$A \rightarrow C$	$C \rightarrow P$
Source+CLIP			69.8	85.2
w/ \mathcal{L}_C	✓		72.7	89.3
w/ \mathcal{L}_V		✓	70.5	85.8
DAM	✓	✓	75.2	89.3

DAM combined with CoreSet and MHPL outperforms their BIAS-integrated counterparts, achieving accuracy gains of 2.4%/7.1%/3.8% and 0.5%/1.7%/0.9% over CoreSet+BIAS and MHPL+BIAS on Office, Office-Home, and VisDA-C, respectively. Notably, DAM surpasses both UDA and ADA methods that require access to source data, confirming the efficacy of leveraging ViL model supervision.

Table 3: Training resource comparison: parameter count and GPU memory usage with (w/) and without (w/o) the ViL model.

w/ ViL	Trainable Params[M]	Peak GPU Memory[GB]
✗ (ours)	24.041 24.043(+0.002)	5.43 5.91(+0.48)

3.5. Ablation Analysis

Our analysis is based on MHPL+DAM framework.

Loss Ablation. To evaluate the individual contributions of the loss components in DAM, we conduct an ablation study on the two losses applied to the ViL model. The results, presented in Table 2, use the direct combination of 'Source+CLIP' as the baseline. Our findings demonstrate the consistent and significant importance of each loss component for the overall performance.

The Ratio ρ of Active Samples. To investigate the impact of the active sample ratio ρ , we conduct experiments on the $A \rightarrow C$ and $C \rightarrow P$ transfer tasks from the Office-Home dataset. As shown in Fig. 2, the performance of MHPL enhanced with DAM consistently and significantly surpasses that of the base MHPL across all tested ratios. Notably, even under limited labeling budgets (i.e., small values of ρ), DAM still delivers substantial performance improvements.

Computational Cost. Table 3 summarizes the computational costs during training. Our DAM framework employs a prompt learning technique, adding merely 0.002M trainable parameters during training and a modest 0.48 GB (8.8%) increase in GPU memory. Notably, the ViL module contributes zero additional FLOPs during inference as it is deactivated post-training, and only the target model is used. This optimized design preserves real-time performance while enhancing model capabilities.

4. CONCLUSION AND FUTURE WORK

Conclusion. We propose DAM, a novel plug-and-play framework for SFADA that enhances and improves supervision by combining sparse human annotations with rich multimodal knowledge from a ViL model via the *Dual-Focused active Supervision*. The adaptation process is optimized using *Alternative Distillation* between the target model and supervisions, which integrates task-specific priors and generalization capabilities. Extensive experiments on multiple benchmarks validate the effectiveness of our method's consistent and substantial improvements over SOTAs.

Future Work. DAM is compatible with various active sampling strategies, yielding different performance outcomes. A promising direction for future work is the exploration of optimal sampling methods within this collaborative architecture. As the present study focuses on ViL activation, we leave the investigation of sampling strategies for future research.

5. REFERENCES

- [1] Chunjiang Ge, Rui Huang, Mixue Xie, Zihang Lai, Shiji Song, Shuang Li, and Gao Huang, “Domain adaptation via prompt learning,” *TNNLS*, vol. 36, no. 1, pp. 1160–1170, 2023.
- [2] Xin Jin, Cuiling Lan, Wenjun Zeng, and Zhibo Chen, “Domain prompt tuning via meta relabeling for unsupervised adversarial adaptation,” *TMM*, vol. 26, pp. 8333–8347, 2024.
- [3] Aditya Golatkar, Alessandro Achille, Yu-Xiang Wang, Aaron Roth, Michael Kearns, and Stefano Soatto, “Mixed differential privacy in computer vision,” in *CVPR*, 2022, pp. 8376–8386.
- [4] Jian Liang, Dapeng Hu, and Jiashi Feng, “Do we really need to access the source data? source hypothesis transfer for unsupervised domain adaptation,” in *ICML*, 2021.
- [5] Haifeng Xia, Handong Zhao, and Zhengming Ding, “Adaptive adversarial network for source-free domain adaptation,” in *ICCV*, 2021, pp. 9010–9019.
- [6] Yuqi Fang, Pew-Thian Yap, Weili Lin, Hongtu Zhu, and Mingxia Liu, “Source-free unsupervised domain adaptation: A survey,” *Neural Netw.*, vol. 174, no. C, 2024.
- [7] Fan Wang, Zhongyi Han, Zhiyan Zhang, Rundong He, and Yilong Yin, “MHPL: Minimum happy points learning for active source free domain adaptation,” in *CVPR*, 2023, pp. 20008–20018.
- [8] Shuang Li, Rui Zhang, Kaixiong Gong, Mixue Xie, Wenxuan Ma, and Guangyu Gao, “Source-free active domain adaptation via augmentation-based sample query and progressive model adaptation,” *TNNLS*, vol. 36, no. 2, pp. 2538–2550, 2023.
- [9] Fan Wang, Zhongyi Han, and Yilong Yin, “Bias: Bridging inactive and active samples for active source free domain adaptation,” *Knowledge-Based Systems*, vol. 284, pp. 111151, 2024.
- [10] Alec Radford, Jong Wook Kim, Chris Hallacy, Aditya Ramesh, Gabriel Goh, Sandhini Agarwal, Girish Sastry, Amanda Askell, Pamela Mishkin, Jack Clark, Gretchen Krueger, and Ilya Sutskever, “Learning transferable visual models from natural language supervision,” in *ICML*, 2021, pp. 8748–8763.
- [11] Chao Jia, Yinfai Yang, Ye Xia, Yi-Ting Chen, Zarana Parekh, Hieu Pham, Quoc V. Le, Yunhsuan Sung, Zhen Li, and Tom Duerig, “Scaling up visual and vision-language representation learning with noisy text supervision,” in *ICML*, 2021, pp. 4904–4916.
- [12] Kaiyang Zhou, Jingkang Yang, Chen Change Loy, and Ziwei Liu, “Learning to prompt for vision-language models,” *IJCV*, vol. 130, no. 9, pp. 2337–2348, 2022.
- [13] Renrui Zhang, Rongyao Fang, Wei Zhang, Peng Gao, Kun-chang Li, Jifeng Dai, Yu Qiao, and Hongsheng Li, “Tip-adapter: Training-free CLIP-adapter for better vision-language modeling,” in *ECCV*, 2022, p. 453–470.
- [14] Song Tang, Wenxin Su, Mao Ye, and Xiatian Zhu, “Source-free domain adaptation with frozen multimodal foundation model,” in *CVPR*, 2024, pp. 23711–23720.
- [15] Xinyao Li, Zhekai Du, Jingjing Li, Lei Zhu, and Ke Lu, “Source-free active domain adaptation via energy-based locality preserving transfer,” in *ACMM*, 2022, pp. 5802–5810.
- [16] Ozan Sener and Silvio Savarese, “ACTIVE LEARNING FOR CONVOLUTIONAL NEURAL NETWORKS: A CORE-SET APPROACH,” in *ICLR*, 2018.
- [17] Kaiyang Zhou, Jingkang Yang, Chen Change Loy, and Ziwei Liu, “Conditional prompt learning for vision-language models,” in *CVPR*, 2022, pp. 16795–16804.
- [18] You Ma, Lin Chai, Shi Tu, and Qingling Wang, “Exploring relational knowledge for source-free domain adaptation,” *TCSVT*, vol. 35, no. 2, pp. 1825–1839, 2025.
- [19] Kate Saenko, Brian Kulis, Mario Fritz, and Trevor Darrell, “Adapting visual category models to new domains.pdf,” in *European Conference on Computer Vision*, 2012, pp. 213–226.
- [20] Hemanth Venkateswara, Jose Eusebio, Shayok Chakraborty, and Sethuraman Panchanathan, “Deep hashing network for unsupervised domain adaptation,” in *CVPR*, 2017, pp. 5385–5394.
- [21] Xingchao Peng, Ben Usman, Neela Kaushik, Judy Hoffman, Dequan Wang, and Kate Saenko, “Visda: The visual domain adaptation challenge,” *ArXiv*, vol. abs/1710.06924, 2017.
- [22] Kaiming He, Xiangyu Zhang, Shaoqing Ren, and Jian Sun, “Deep residual learning for image recognition,” in *CVPR*, 2016, pp. 770–778.
- [23] Alexey Dosovitskiy, Lucas Beyer, Alexander Kolesnikov, Dirk Weissenborn, Xiaohua Zhai, Thomas Unterthiner, Mostafa Dehghani, Matthias Minderer, Georg Heigold, Sylvain Gelly, Jakob Uszkoreit, and Neil Houlsby, “An image is worth 16x16 words: Transformers for image recognition at scale,” in *ICLR*, 2021.
- [24] Zhen Qiu, Yifan Zhang, Hongbin Lin, Shuaicheng Niu, Yanxia Liu, Qing Du, and Mingkui Tan, “Source-free domain adaptation via avatar prototype generation and adaptation,” in *IJCAI*, 2021, pp. 2921–2927.
- [25] Viraj Prabhu, Arjun Chandrasekaran, Kate Saenko, and Judy Hoffman, “Active domain adaptation via clustering uncertainty-weighted embeddings,” in *ICCV*, 2021, pp. 8485–8494.
- [26] Binhui Xie, Longhui Yuan, Shuang Li, Chi Harold Liu, Xining Cheng, and Guoren Wang, “Active learning for domain adaptation: An energy-based approach,” in *AAAI*, 2022, pp. 8708–8716.
- [27] Mixue Xie, Shuang Li, Rui Zhang, and Chi Harold Liu, “DIRICHLET-BASED UNCERTAINTY CALIBRATION FOR ACTIVE DOMAIN ADAPTATION,” in *ICLR*, 2023.
- [28] Wenxiao Xiao, Jiuxiang Gu, and Hongfu Liu, “Category-aware active domain adaptation,” in *ICML*, 2024, pp. 54276–54287.